Christiansson, A., Gutman, H., Wieslander, Å., & Lindblom, G. (1981) *Biochim. Biophys. Acta 645*, 24-32.
Christiansson, E., Eriksson, L. E. G., Westman, J., Demel, R., & Wieslander, Å. (1985) *J. Biol. Chem. 260*, 3984-3990.
Crowley, J. M. (1973) *Biophys. J. 13*, 711-724.
Donohue-Rolfe, A. M., & Schaechter, M. (1980) *Proc. Natl. Acad. Sci. U.S.A. 77*, 1867-1871.
Hartree, E. F. (1972) *Anal. Biochem. 48*, 422-427.
Hopper, U., Lehninger, A. L., & Lennartz, W. J. (1970) *J. Membr. Biol. 2*, 41-58.
Langley, K. E., & Kennedy, E. P. (1979) *Proc. Natl. Acad. Sci. U.S.A. 76*, 6245-6249.
LeGrimellec, C., Lajeunesse, D., & Rigaud, J.-L. (1982) *Biochim. Biophys. Acta 687*, 281-290.
Lelkes, P. I. (1979) *Biochem. Biophys. Res. Commun. 90*, 656-662.
Liberman, E. A., Topaly, V. P., Tsofina, L. M., Jasaitis, A. A., & Skulachev, V. P. (1969) *Nature (London) 222*, 1076-1078.
Lubin, M. (1964) *Fed. Proc., Fed. Am. Soc. Exp. Biol. 23*, 994-1001.
Padan, E., Zilberstein, D., & Schuldiner, S. (1981) *Biochim. Biophys. Acta 650*, 151-166.
Pollack, J. D., Tryon, V. V., & Beaman, K. D. (1983) *Yale J. Biol. Med. 56*, 709-716.
Pressman, B. C. (1976) *Annu. Rev. Biochem. 45*, 501-530.
Reed, P. W. (1979) *Methods Enzymol. 55*, 435-454.
Rilfors, L. (1985) *Biochim. Biophys. Acta 813*, 151-160.
Rilfors, L., Lindblom, G., Wieslander, Å., & Christiansson, A. (1984) *Biomembranes 12*, 205-245.
Robillard, G. T., & Konings, W. N. (1982) *Eur. J. Biochem. 127*, 597-604.
Rottem, S., Linker, C., & Wilson, T. H. (1981) *J. Bacteriol. 145*, 1299-1304.
Rottenberg, H. (1979) *Methods Enzymol. 55*, 547-569.
Shchipunov, Yu. A., & Drachev, G. Yu. (1982) *Biochim. Biophys. Acta 691*, 353-358.
Smith, P. F. (1969) *J. Bacteriol. 99*, 480-486.
Sugar, I. P. (1979) *Biochim. Biophys. Acta 556*, 72-85.
Sugar, I. P. (1982) *Biophys. Chem. 15*, 131-138.
Van Echteld, C. J. A., Van Stigt, R., de Kruijff, B., Leunissen-Bijvelt, J., Verkleij, A., & de Gier, J. (1981) *Biochim. Biophys. Acta 648*, 287-291.
Waddell, W. J., & Butler, T. C. (1959) *J. Clin. Invest. 38*, 720-729.
Wieslander, Å., Christiansson, A., Rilfors, L., & Lindblom, G. (1980) *Biochemistry 19*, 3650-3655.
Wieslander, Å., Christiansson, A., Rilfors, L., Johansson, L., Khan, A., & Lindblom, G. (1981) *FEBS Lett. 124*, 273-278.
Wieslander, Å., Rilfors, L., & Lindblom, G. (1986) *Biochemistry* (submitted for publication).
Zaritsky, A., & Macnab, R. M. (1981) *J. Bacteriol. 147*, 1054-1062.

Correlation between Acetylcholine Receptor Function and Structural Properties of Membranes†

Tung Ming Fong and Mark G. McNamee*
Department of Biochemistry and Biophysics, University of California, Davis, California 95616
Received July 17, 1985

ABSTRACT: Protein-lipid interactions were studied by using *Torpedo californica* acetylcholine receptor (AChR) as a model system by reconstituting purified AChR into membranes containing various synthetic lipids and native lipids. AChR function was determined by measuring two activities at 4 °C: (1) low to high agonist affinity-state transition of AChR in the presence of an agonist (carbamylcholine) in either membrane fragments or sealed vesicles and (2) ion-gating activity of AChR-containing vesicles in response to carbamylcholine. Sixteen samples were examined, each containing different lipid compositions including phosphatidylcholine, cholesterol, phosphatidic acid, phosphatidylethanolamine, asolectin, neutral lipid depleted asolectin, native lipids, and cholesterol-depleted native lipids. Phosphatidylcholines with different configurations of fatty acyl chains were used. The dynamic structures of these membranes were probed by incorporating spin-labeled fatty acid into AChR-containing vesicles and measuring the order parameters. It was found that both aspects of AChR function were highly dependent on the lipid environment even though carbamylcholine binding itself was not affected. An appropriate membrane fluidity was necessarily required to allow the interconversion between the low and high affinity states of AChR. An optimal fluidity hypothesis is proposed to account for the conformational transition properties of membrane proteins. In addition, the conformational change was only a necessary, but not sufficient, condition for the AChR-mediated ion flux activity. Among membranes in which AChR manifested the affinity-state transition, only those containing both cholesterol and negatively charged phospholipids (such as phosphatidic acid) retained the ion-gating activity.

The interactions between membrane proteins and lipids have been studied by various magnetic resonance (Griffith et al., 1982; Devaux, 1983) and fluorescence techniques (London & Feigenson, 1981; Pink et al., 1984). Many recent discoveries have led to the notion that membrane lipids are not only a structural component of cellular compartmentation but also a functionally important element involved in some biological functions of membrane proteins. However, only a few experiments provide a direct link between the specific biochem-

† This work was supported by Grant NS13050 from the National Institute of Neurological and Communicative Disorders and Stroke awarded to M. G.M. and by a Jastro-Shields Graduate Research Scholarship and a Henry A. Jastro Fellowship from the University of California at Davis to T.M.F.

0006-2960/86/0425-0830$01.50/0

ical functions of membrane proteins and the structural and dynamic properties of membrane lipids. With respect to the dynamic structure of membranes, there is evidence that the membrane fluidity may play an important role in some biological functions such as anesthesia, aging, cell growth, and differentiation [see Yguerabide & Yguerabide (1985)]. Membrane fluidity is a semiquantitative term encompassing all molecular motions throughout the membrane bilayer such as lateral and rotational motions, trans–gauche isomerizations, and anisotropic motions. Scandella et al. (1982) reported that a marked decrease in the order parameter of sea urchin egg membranes was associated with fertilization. It was also demonstrated that plasma membranes from Duchenne dystrophy human skin fibroblasts showed significantly less order than control fibroblasts (Shaw et al., 1983).

In several cases, specific lipid molecules are found to be critical for membrane enzymes. It has been shown that cholesterol inhibited the catalytic activity of Ca^{2+}-ATPase[1] (Warren et al., 1975), while in parallel it was demonstrated that Ca^{2+}-ATPase interacted very weakly with cholesterol in membranes (Silvius et al., 1984; Simmonds et al., 1984). In contrast, it was shown that a critical concentration of cholesterol was required for the maximal catalytic activity of adenylate cyclase (Whetton et al., 1983a,b). However, no hypothesis in terms of molecular interactions and protein conformation has been proposed to account for the lipid requirement [see Marsh (1983) and Sandermann (1983)]. Many previous experiments have not provided a correlation between specific function and the dynamic structure of membranes, mainly due to the lack of a chemically defined model system which is required for any study of lipid–protein interactions.

Acetylcholine receptor (AChR) from the electric ray *Torpedo californica* has been purified and reconstituted into defined lipid environments (McNamee & Ochoa, 1982), thus providing an excellent model system for studying protein–lipid interactions. The *Torpedo* AChR is a pentameric integral membrane protein involved in cholinergic synaptic transmission (Changeux et al., 1984). Substantial efforts have been focused on elucidating the molecular mechanism of AChR function [see Barrantes (1983), Hess et al. (1983), Popot & Changeux (1984), and McNamee et al. (1986)], and three aspects of AChR function have been studied in detail: (1) the binding of specific agonists; (2) the activation of a cation channel upon agonist binding; and (3) the desensitization process by which ion permeability becomes blocked in the prolonged presence of activating agonist. These different biochemical processes can be studied separately, making it possible to correlate specific functions of AChR with the structural properties of the lipid environment.

Previous results have demonstrated that membrane lipids interact differentially with AChR. For example, sterol, phosphatidic acid (PA), and fatty acid spin-labels have a relatively high affinity for AChR compared to other kinds of spin-labeled phospholipids (Ellena et al., 1983). Biochemical studies have also shown that the ion-gating activity of AChR is very sensitive to the lipid environment. For example, cholesterol (CH) and negatively charged phospholipids such as PA are required to support the ion-gating activity (Dalziel et al., 1980; Ochoa et al., 1983; Criado et al., 1984). In contrast, unsaturated free fatty acids were found to inhibit AChR-mediated ion flux, which is attributable to the perturbation of the functionally important interactions between AChR and cholesterol and/or negatively charged phospholipids (Andreasen & McNamee, 1980; Pjura et al., 1982). Another interesting aspect of AChR function is the desensitization process which is correlated to the equilibrium shift of AChR from a low agonist affinity state to a high-affinity state (Weber et al., 1975; Weiland et al., 1977; Quast et al., 1978). This process, like channel opening, also involves conformational changes that can be affected by the dynamic properties of the lipid environment.

We report here the effects of membrane fluidity on the conformational changes involved in the functioning of AChR including both the affinity-state transition and the ion-gating event. We confirm the requirement of cholesterol and negatively charged phospholipids for supporting the ion-gating activity. These results are interpreted in the context of two general hypotheses that may be applicable to other systems; i.e., the conformational transition of membrane proteins requires an optimal fluidity, and cholesterol may stabilize the α-helical structure in membrane proteins.

Materials and Methods

Acetylcholine Receptor Purification and Reconstitution. AChR-rich membranes were prepared from 600 g of frozen *Torpedo californica* electroplax as described by Ochoa et al. (1983) with a slight modification of buffer A (100 mM NaCl–10 mM MOPS–0.1 mM EDTA–0.02% NaN_3, pH 7.4). AChR was purified from AChR-rich membranes by affinity chromatography (Ellena et al., 1983), and the native lipids were replaced by synthetic phosphatidylcholine (PC) at the same time. Briefly, cholate-solubilized membranes (2 mg/mL protein and 1% cholate in buffer A) were applied to 50 mL of carboxymethylcholine-derivatized Affi-gel 401 (Bio-Rad, Richmond, CA), and the column was washed with 4 column bed volumes of a solution containing 1 mg/mL dioleoylphosphatidylcholine (DOPC)–1% cholate in buffer A. The column was then washed and equilibrated 3 times with 1 column bed volume of 2.5 mg/mL DOPC–1% cholate, allowing 4-h intervals for equilibration. The column was finally washed with 3 column bed volumes of 0.1–0.4 mg/mL DOPC–0.5% cholate in buffer A. The exact DOPC concentration at this stage determines the lipid:protein ratio (molar ratio) of the final eluate. Pure AChR in DOPC was eluted with 10 mM carbamylcholine (Carb) in the same washing buffer. The protein concentration in each fraction was determined by A_{280}, and fractions required to achieve a certain lipid:protein ratio in the range of 100–400 were pooled and dialyzed. Typical reconstituted membranes had a protein concentration of about 1 mg/mL. In the process of purification and reconstitution, other PC's can be used in the place of DOPC. All synthetic phospholipids and egg PA were obtained from Avanti Polar Lipids (Birmingham, AL). Asolectin was obtained from Associated Concentrates (Woodside, NY).

Extraction of Native Lipids and Removal of Neutral Lipids. Native lipids from *Torpedo* electroplax plasma membranes were extracted by the procedure of Bligh & Dyer (1959) with a slight modification. Before filtration, the homogenate was centrifuged briefly to separate the denatured proteins and other residues from both the aqueous phase and the organic phase. The extracted lipids were analyzed by thin-layer chromatography (Baker-flex silica gel IB-F from Baker Chemical Co.,

[1] Abbreviations: AChR, acetylcholine receptor; ATPase, adenosinetriphosphatase; Carb, carbamylcholine chloride; CH, cholesterol; EDTA, ethylenediaminetetraacetic acid; DEPC, dielaidoylphosphatidylcholine; DLPC, dilinoleoylphosphatidylcholine; DOPC, dioleoylphosphatidylcholine; DOPE, dioleoylphosphatidylethanolamine; DPePC, dipalmitelaidoylphosphatidylcholine; EPR, electron paramagnetic resonance; ^{125}I-BgTx, ^{125}I-monoiodinated α-bungarotoxin; MOPS, 3-(*N*-morpholino)propanesulfonic acid; PA, phosphatidic acid; PC, phosphatidylcholine; BSA, bovine serum albumin.

Phillipsburg, NJ) in $CHCl_3$–MeOH–H_2O–NH_3 (65:25:4:1 v/v). Removal of cholesterol and other neutral lipids was carried out by applying the lipids in $CHCl_3$ to a silica gel (Unisil activated silicic acid from Clarkson Chemical Co., Williamsport, PA) column followed by washing with $CHCl_3$. The remaining lipids were eluted with $CHCl_3$–MeOH (1:1).

Re-reconstitution of AChR in Complex Membranes with a Low Lipid:Protein Ratio. To prepare membrane samples containing a mixture of two or three lipid components, the reconstituted membranes with a lipid:protein ratio of 100:1 in 0.5% cholate were combined with a minimal volume (about 10% of the volume of the reconstituted membranes) of a solution containing the desired lipids in 0.5% cholate to achieve a lipid:protein ratio up to 400:1, equilibrated at 4 °C for 30 min, and dialyzed against 4 L of buffer A for 48 h with three changes of buffer.

Re-reconstitution of AChR in Vesicles with a High Lipid:Protein Ratio. To prepare vesicle samples with a lipid:protein ratio of 10000:1, the desired amount of lipids in a minimal volume (about 20% of the volume of the low lipid:protein ratio sample) of cholate solution was added slowly with gentle stirring to the low lipid:protein ratio sample to achieve a final cholate concentration of 2%. The solution was equilibrated at 4 °C for 30 min and dialyzed against buffer A as described above.

Sucrose Gradient Equilibrium Sedimentation. Membrane samples with low lipid:protein ratios were analyzed in a 20–50% sucrose gradient in buffer A (Ellena et al., 1983), while vesicle samples with high lipid:protein ratios were analyzed in a 5–20% sucrose gradient (Ochoa et al., 1983). The samples were centrifuged at 55000 rpm for 36 h in a Beckman SW-60 rotor (320000*g*). Aliquots of 200 μL were fractionated from each gradient and assayed for AChR and lipid concentrations.

Determination of Toxin Binding Sites on AChR. Equilibrium binding of ^{125}I-monoiodinated α-bungarotoxin (^{125}I-BgTx) (Amersham) in Triton X-100 was measured by using DEAE filters (Schmidt & Raftery, 1973) with the following modifications. Membrane samples containing about 2 pmol of toxin sites were incubated with 7.5 pmol of ^{125}I-BgTx in NMT-100 buffer (100 mM NaCl–10 mM MOPS–0.2% Triton X-100, pH 7.4) for 60 min at room temperature (total volume 65 μL). The incubation mixture was then diluted with 5 mL of NMT-10 buffer (10 mM NaCl–10 mM MOPS–0.2% Triton X-100, pH 7.4) and filtered through two Whatman DE-81 filter disks. The disks were washed with 20 mL of NMT-10 buffer and counted directly in a Packard γ scintillation counter.

Manual Ion Flux Assays. Influx of $^{86}Rb^+$ (New England Nuclear) into AChR-containing vesicles was measured by the method of Walker et al. (1982). In a typical assay, 50 μL of vesicle sample was mixed with 15 μL of a 0.5–1 μCi/μL Rb^+ solution with or without 4.33 mM Carb. Influx was allowed to proceed at a specific temperature (usually 4 °C) for 30 s, and then a 50-μL aliquot was applied to a 2-mL disposable Dowex 50W X8 column and eluted with 3 mL of salt-free 175 mM sucrose solution. The eluate containing trapped Rb^+ in vesicles was collected in scintillation vials and counted in a Beckman LS-3133P liquid scintillation counter without scintillation fluor in the 0-600 window. The total internal volume of the vesicle population was determined by allowing the influx reaction to proceed for 48 h.

Toxin Binding Rate Measurements. The pseudo-first-order association rate constant of α-bungarotoxin to AChR was measured in the absence of detergent but in the presence of bovine serum albumin to prevent aggregation of toxin molecules as described by Walker et al. (1981). An AChR membrane sample (5 nM in toxin sites) was reacted with 30 nM ^{125}I-BgTx in 700 μL of buffer A containing 0.5 mg/mL BSA at room temperature. Three toxin binding reactions were carried out for each membrane sample. (1) The control reaction had no Carb in the reaction mixture, and the reaction was started by adding 50 μL of 70 nM (toxin site concentration) AChR to the toxin solution. (2) The coincubation reaction mixture contained an appropriate concentration of Carb, and the reaction was started by adding 50 μL of AChR sample as above. (3) The preincubation experiment was carried out by first incubating the AChR sample (70 nM in toxin sites) with an equal volume of Carb solution (usually 5 μM) at a specific temperature (usually 4 °C) for 20 min, and then the binding reaction was started by adding 100 μL of the preincubation mixture to the reaction mixture with the same final concentrations of ^{125}I-BgTx and Carb as in the coincubation reaction. The concentration of Carb in the preincubation mixture will determine the minimal concentration of Carb that can be used in the binding reaction.

The Carb dissociation constants were determined by varying the final Carb concentration in the 700-μL reaction mixture from 0.01 μM to 10 mM. The ratio of the observed pseudo-first-order binding rate constant in the presence of Carb (k) to the rate constant in the absence of Carb (k_{max}) was plotted vs. the Carb concentration for both the coincubation and preincubation experiments, respectively. Nonlinear curve fitting of these data provides the Carb binding affinity and the fraction of AChR in the low-affinity state. A Fortran program implemented with the Monte Carlo algorithm was used to perform the nonlinear curve fitting on a VAX-11/785 computer.

Incorporation of Spin-Labeled Fatty Acid into Membranes and EPR Spectroscopy. Fifteen nanomoles of 5-doxylhexadecanoic acid (Aldrich) in ethanol was dried at the bottom of a cryotube with a stream of argon gas. Fifty microliters of AChR-containing vesicle sample was added to the cryotube while vortexing, and the tube was freeze–thawed in liquid nitrogen at least 3 times to ensure incorporation of spin-labeled fatty acid into membranes. The vesicle suspension was aspirated into a capillary tube, and the EPR spectrum was recorded on a Varian E-3 X-band EPR spectrometer equipped with a temperature-control unit. Spectra were recorded with modulation frequency at 100 kHz, modulation amplitude at 1.0 G, microwave power at 8 mW, and midfield magnetic field strength at 3238 G. Order parameters were calculated from the spectral splittings as described by Gaffney (1976).

Other Assays. Phospholipids were determined by organic phosphorus content (McClare, 1971) or phosphatidylcholine content (Yoshida et al., 1980). Protein concentration was determined by the Lowry method (Lowry et al., 1951). Cholesterol concentration was determined by the colorimetric assay kit from Boehringer Mannheim (Indianapolis, IN) or by including [^{14}C]cholesterol (New England Nuclear) during reconstitution.

RESULTS

Physical Properties of the Reconstituted Membranes and Vesicles. It has been shown that AChR in reconstituted PC membranes at a low lipid:protein ratio (100–400) is indeed associated with phospholipids (Ellena et al., 1983). To verify that the same situation holds true in re-reconstituted membranes supplemented with additional lipids, re-reconstituted AChR–DOPC–CH (1:200:200) membranes were analyzed by 20–50% sucrose gradient equilibrium sedimentation. As shown

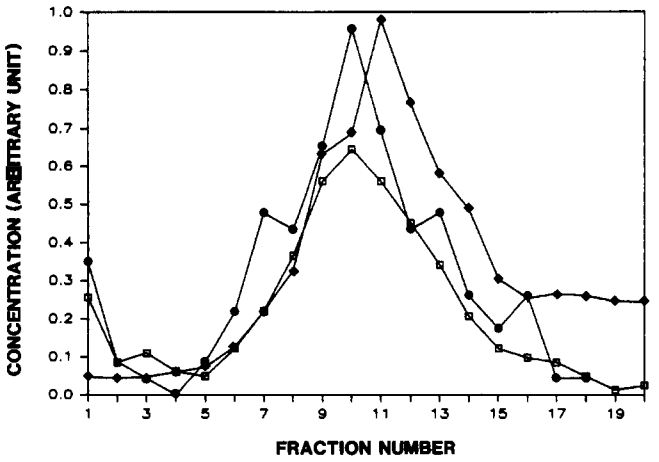

FIGURE 1: Sucrose gradient (20–50%) equilibrium sedimentation analysis of re-reconstituted membranes containing AChR–DOPC–CH (1:200:200 mol/mol). (♦) AChR concentration determined by ^{125}I-BgTx equilibrium binding assay; (●) CH concentration determined by enzymatic cholesterol assay; (□) PC concentration.

in Figure 1, only one population of membrane fragments was found, in which AChR was firmly associated with both DOPC and CH. Transmission electron microscopy also demonstrated that these reconstituted AChR membranes with a low lipid:protein ratio were in the form of membrane fragments (J. P. Earnest and M. G. McNamee, unpublished results).

For the AChR-containing vesicle samples prepared at high lipid:protein ratios, a slightly different situation was observed. Immediately after dialysis, nonfrozen vesicle samples (e.g., AChR–DOPC and AChR–DOPC–PA–CH) were analyzed by 5–20% sucrose gradient equilibrium sedimentation. Two populations of vesicles were obtained as shown in Figure 2A,C, one of which contained liposomes without AChR. After several cycles of freeze–thawing in liquid nitrogen, however, a more homogeneous population of vesicles containing AChR and lipids was obtained (Figure 2B,D). Freeze–thaw cycles clearly increased the homogeneity of the vesicle population with respect to AChR distribution as previously reported by Anholt et al. (1982). On the basis of this observation, only frozen vesicle samples were used in the following experiments. It should be pointed out that the distribution of AChR on the vesicle surface may be more complicated than what can be determined by the gradient sedimentation analysis (J. P. Earnest and M. G. McNamee, unpublished experiments).

The orientation of AChR in vesicles was determined by measuring the total toxin binding sites in the presence of Triton X-100 and the right-side-out toxin binding sites in the absence of detergent. It was found that 85–95% of AChR's were right-side-out for all reconstituted vesicle samples (data not shown).

Carbamylcholine Binding to AChR in Different Lipid Environments. The binding affinity of Carb for AChR was determined by a competition assay in which the pseudo-first-order association rate constant of ^{125}I-BgTx and AChR was measured in the presence of Carb (Quast et al., 1978; Walker et al., 1981). The toxin binding rate assay is especially useful for studying the effects of lipid environments since the

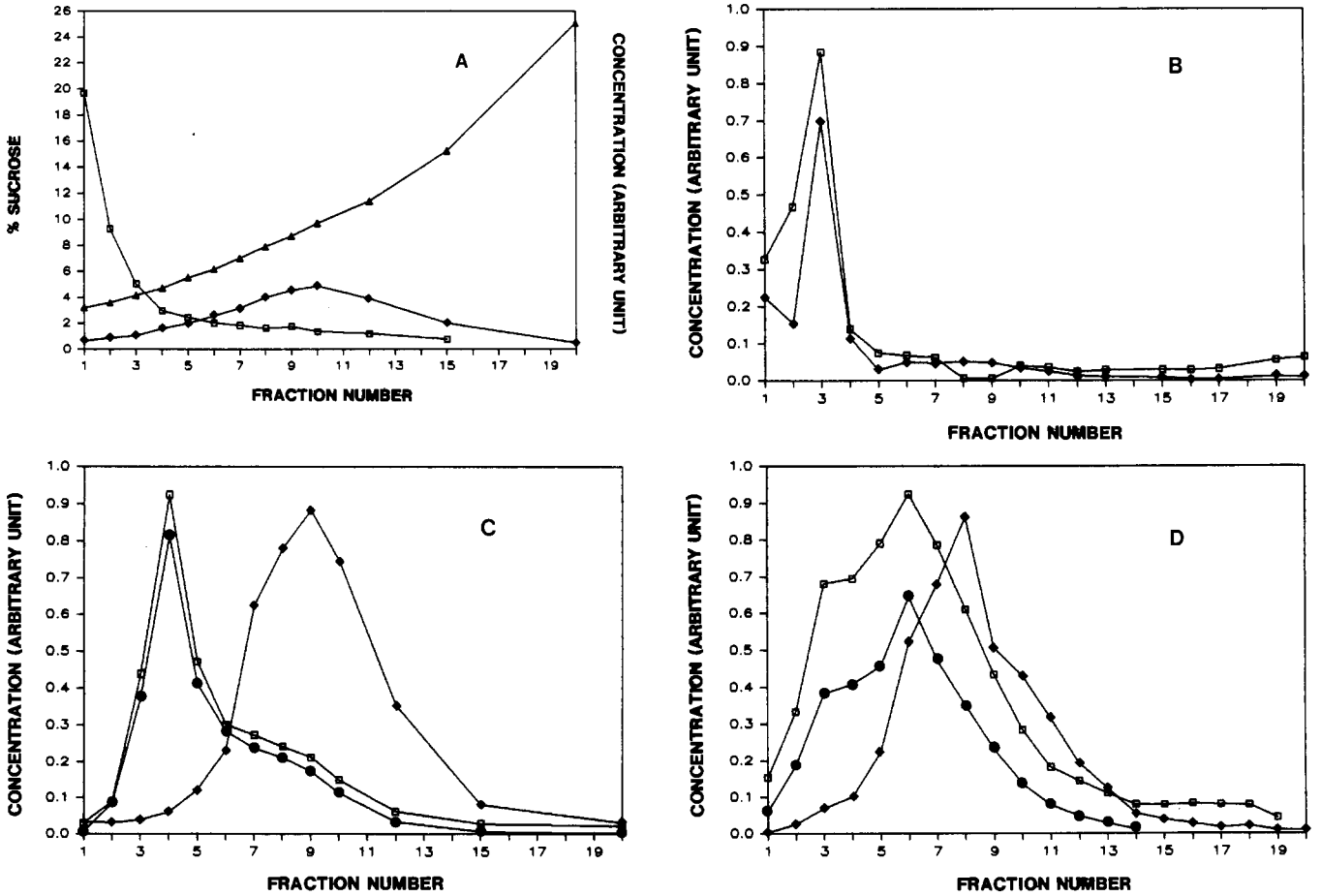

FIGURE 2: Sucrose gradient (5–20%) equilibrium sedimentation analysis of re-reconstituted AChR-containing vesicles. (▲) Percent sucrose (w/w) determined by the refractive index; (□) PC concentration; (♦) AChR concentration determined by ^{125}I-BgTx equilibrium binding assay; (●) cholesterol concentration determined by [^{14}C]cholesterol amounts. (A) Unfrozen AChR–DOPC vesicles; (B) frozen AChR–DOPC vesicles; (C) unfrozen AChR–DOPC–PA–CH vesicles; (D) frozen AChR–DOPC–PA–CH vesicles.

Table I: Equilibrium Properties of AChR in Different Lipid Environments[a]

membrane lipids	Carb dissociation constants (M)		fraction of low-affinity-state AChR				
	K_1	K_2	−Carb	+Carb[b]	K_c	K_{c1}	K_{c2}
DOPC	7.4×10^{-5}	3.8×10^{-7}	0.45	0.45 (6.7 μM)			
DOPC–CH (75:25)	7.8×10^{-5}	9.1×10^{-8}	0.68	0.68 (2.5 μM)			
DOPC–PA–CH (56:19:25)	8.3×10^{-5}	6.4×10^{-7}	0.88	0.48 (3.5 μM)	7.1	0.055	4.2×10^{-4}
asolectin	1.6×10^{-5}	5.4×10^{-8}	0.63	0.28 (0.35 μM)	1.7	0.059	2.0×10^{-5}

[a] The constants K_1, K_2, K_c, K_{c1}, and K_{c2} are defined in Figure 5. [b] The values enclosed in parentheses are the Carb concentration present in the preincubation mixture.

formation of sealed vesicles is not required. Both reconstituted membranes with a low lipid:protein ratio (160–400) and reconstituted vesicles with a high lipid:protein ratio gave the same results from the toxin binding rate assay (see Table II, e.g., AChR–DEPC system). For membranes with more than one lipid component, however, the change of the lipid:protein ratio will result in a change in the lipid composition of the bulk-phase lipid domain [see equations derived by Brotherus et al. (1981)]. Such changes in lipid composition can be ignored if the lipid:protein ratio is not very close to the number of lipid molecules surrounding the membrane protein (i.e., lipid:protein ratio > 400). Therefore, both types of samples were used in the toxin binding rate assays. Two typical experiments are shown in Figure 3 for the specific concentration of Carb used in the binding assay. Pseudo-first-order association rate constants were calculated for each binding curve by linear least-squares regression analysis. AChR in DOPC membranes did not manifest the characteristic low-affinity- to high-affinity-state transition upon preincubation with Carb (Figure 3A) since the rate constant of ^{125}I-BgTx binding to AChR in the presence of Carb was not significantly different from that of ^{125}I-BgTx binding to AChR preincubated with Carb (see Table II). In contrast, AChR in DOPC–PA–CH membranes was completely functional with respect to the conformational change (Figure 3B). The difference in k_{max}'s for different samples was due to the slight variation of ^{125}I-BgTx concentration in each batch and/or the slight variation of AChR concentration. However, the exact values of k_{max}, k_{co} (coincubation experiment), and k_{pre} (preincubation experiment) are not critical in evaluating the agonist binding affinity because it is the ratios of k_{co}/k_{max} and k_{pre}/k_{max} that are used in the curve fitting to obtain the agonist dissociation constants. When the toxin binding rate measurements were carried out for different Carb concentrations, the results of k/k_{max} were plotted as a function of [Carb] as shown in Figure 4. Nonlinear least-squares curve fitting was performed by using the Monte Carlo algorithm to obtain the best fit for the equation

$$k/k_{max} = \frac{F_a}{1 + [Carb]/K_1} + \frac{1 - F_a}{1 + [Carb]/K_2} \quad (1)$$

which is derived according to the model shown in Figure 5. In the cases of AChR–DOPC and AChR–DOPC–CH in which AChR did not manifest the equilibrium shift of agonist affinity state upon preincubation with agonist, both coincubation and preincubation data were fitted to a single equation. For AChR–DOPC–PA–CH and AChR–asolectin, however, coincubation and preincubation data were fitted respectively to two different equations having different F_a values but the same K_1 and K_2 values using the simultaneous curve-fitting procedure (De Lean et al., 1978). F_a is the fraction of AChR having an agonist binding affinity of K_1, and it is dependent on the concentration of Carb in the preincubation mixture. From the values of K_1, K_2, and F_a, the equilibrium constants for the affinity-state interconversion, i.e., K_c, K_{c1}, and K_{c2}, can be calculated. As shown in Table I, the agonist binding affinity itself is not sensitive to the change of lipid environment, but the affinity-state interconversion is highly dependent on the nature of membranes.

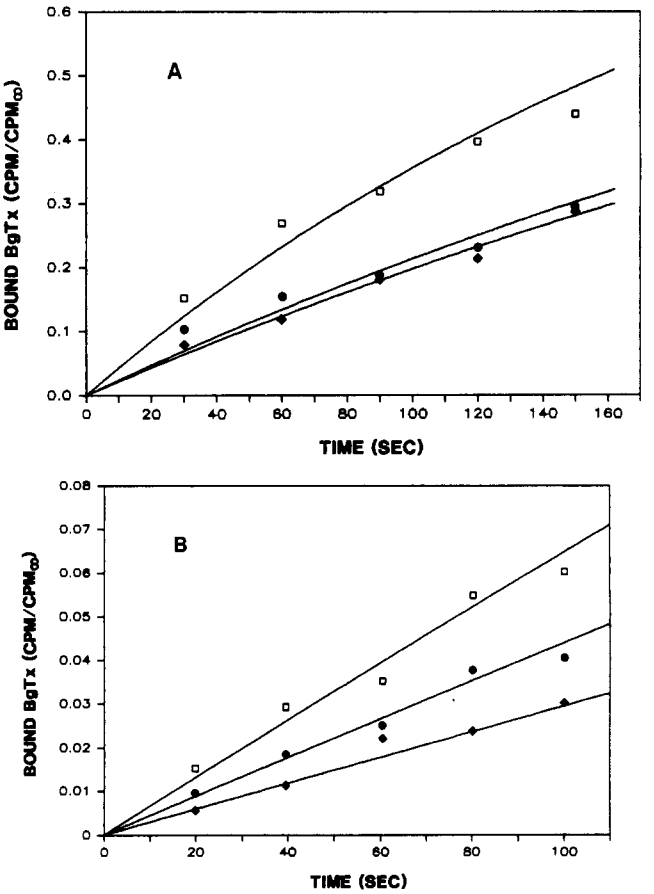

FIGURE 3: Time course of ^{125}I-BgTx binding to reconstituted AChR membranes. Solid lines were calculated from the first-order rate equation. (A) Reconstituted AChR–DOPC membranes (lipid:protein ratio = 400). (□) In the absence of Carb, $k_{max} = 0.0044$ s^{-1}; (●) in the presence of 5 μM Carb, $k_{co} = 0.0024$ s^{-1}; (♦) AChR was preincubated in 2.5 μM Carb for 20 min at 4 °C, and the binding was then measured in the presence of 5 μM Carb, $k_{pre} = 0.0022$ s^{-1}. (B) Re-reconstituted AChR–DOPC–PA–CH vesicles. (□) In the absence of Carb, $k_{max} = 0.00067$ s^{-1}; (●) in the presence of 5 μM Carb, $k_{co} = 0.00045$ s^{-1}; (♦) AChR was preincubated in 2.5 μM Carb, and the binding was then measured in the presence of 5 μM Carb, $k_{pre} = 0.00030$ s^{-1}.

Affinity-State Interconversion of AChR in Different Lipid Environments. It is not necessary to construct a complete dose–response curve, such as those in Figure 4, to determine whether AChR is capable of undergoing the affinity-state transition. One concentration of Carb (e.g., 5 μM) approximately in the middle of the dose–response curve was chosen so that k_{co} would differ from k_{pre} if AChR were able to undergo conformational changes. Table II lists the values of ^{125}I-BgTx binding rate constants to AChR in various membranes. A *t*

Table II: Toxin Binding Rate Constants for AChR Reconstituted in Different Lipid Environments

lipids[a]	toxin binding rate constants ($\times 10^{-3}$ s^{-1})[b] k_{max}	k_{5co}	$k_{2.5pre,5co}$	t test[c]
DOPC ($1/p$ = 400)	3.95 ± 0.24 (2)	2.39 ± 0.06 (2)	2.59 ± 0.59 (2)	p = 0.35
DOPC–CH (200:200)	4.47 ± 1.22 (2)	3.68 ± 0.67 (2)	2.64 ± 0.06 (2)	p = 0.07
DOPC–PA–CH[d]	0.91 ± 0.11 (2)	0.73 ± 0.13 (2)	0.54 ± 0.05 (2)	p = 0.09
	0.84 ± 0.01 (2)	0.43 ± 0.14 (2)	0.22 ± 0.01 (2)	p = 0.07 (23 °C)
asolectin	1.43 ± 0.73 (2)	0.61 ± 0.19 (2)	0.39 ± 0.001 (2)	p = 0.12
neutral lipid depleted asolectin	2.02 ± 0.30 (2)	1.47 ± 0.01 (2)	1.36 ± 0.01 (2)	p = 0.005
DLPC–PA–CH[d]	2.22 ± 0.10 (2)	1.28 ± 0.17 (2)	1.19 ± 0.10 (2)	p = 0.30
DEPC ($1/p$ = 160)	3.24 ± 1.23 (4)	2.61 ± 0.44 (4)	1.65 ± 0.56 (4)	p = 0.02
DEPC	3.91 ± 0.41 (2)	3.37 ± 0.28 (2)	2.67 ± 0.34 (2)	p = 0.07
DEPC–CH (3:1)	3.58 ± 1.05 (4)	2.41 ± 0.39 (4)	2.48 ± 0.16 (3)	p = 0.37
DEPC–CH (6:4)	7.34 ± 1.65 (4)	5.16 ± 1.56 (3)	4.52 ± 0.28 (3)	p = 0.28
DEPC–PA–CH[d]	3.92 ± 0.13 (4)	2.97 ± 0.91 (4)	2.85 ± 0.90 (3)	p = 0.41
	1.16 ± 0.17 (2)	0.80 ± 0.03 (2)	0.56 ± 0.12 (2)	p = 0.06 (15 °C)
DPePC–PA–CH[d]	2.45 ± 0.41 (2)	2.18 ± 0.01 (2)	1.92 ± 0.10 (2)	p = 0.12
DPePC–DOPE–CH[d]	2.31 ± 0.31 (5)	1.48 ± 0.20 (4)	1.18 ± 0.07 (4)	p = 0.02
DPePC–CH (3:1)	1.37 ± 0.87 (6)	1.23 ± 0.66 (6)	1.08 ± 0.56 (5)	p = 0.35
CH-depleted *Torpedo* lipids	1.79 ± 0.12 (4)	1.12 ± 0.21 (4)	1.08 ± 0.19 (4)	p = 0.38

lipids[a]	toxin binding rate constants ($\times 10^{-3}$ s^{-1})[b] k_{max}	k_{5co}	$k_{10pre,5co}$	t test[c]
Torpedo lipids	3.63 ± 0.35 (2)	2.47 ± 0.07 (2)	1.82 ± 0.18 (2)	p = 0.02
DOPC–CH (2.24:1)	2.61 ± 0.23 (2)	2.20 ± 0.46 (2)	2.36 ± 0.77 (2)	p = 0.41

lipids[a]	toxin binding rate constants ($\times 10^{-3}$ s^{-1})[b] k_{max}	k_{10co}	$k_{2.5pre,10co}$	t test[c]
DOPC–CH (2.24:1)	3.32 ± 0.73 (2)	2.45 ± 0.34 (2)	2.43 ± 0.10 (2)	p = 0.47

[a] Abbreviations: DEPC, dielaidoylphosphatidylcholine; DLPC, dilinoleoylphosphatidylcholine; DOPC, dioleoylphosphatidylcholine; DOPE, dioleoylphosphatidylethanolamine; DPePC, dipalmitelaidoylphosphatidylcholine. All samples are high lipid to protein ratio vesicles ($1/p$ = 10000) unless indicated in parentheses. [b] k_{max} is the pseudo-first-order rate constant in the absence of Carb. k_{5co} is the rate constant in the presence of Carb whose concentration is indicated by the subscript in units of micromolar and in which the subscript "co" denotes coincubation. $k_{2.5pre,5co}$ is the rate constant for AChR having been preincubated with the indicated concentration of Carb. All preincubations were carried out at 4 °C unless indicated in the table. [c] Student's t test of the level of significant difference between k_{co} and k_{pre}. The probability of the null hypothesis is listed. [d] The ratio is 56:19:25.

Table III: Ion-Gating Properties of AChR-Containing Vesicles[a]

lipids	−Carb ($\times 10^3$ cpm)	+Carb (30 s) $\times 10^3$ cpm	IV (μL/mL)	EIV (μL/mL)	response[b] ($\times 10^{-2}$ μM^{-1})
Torpedo	6.4 ± 1.2	11.3 ± 1.5	2.7	6.9	6.0
CH-depleted *Torpedo*	2.6 ± 1.0	5.4 ± 1.9	1.4	14.7	0.7
DEPC	24.7 ± 7.0	24.5 ± 1.4	9.5	7.1	
	5.6 ± 0.9	4.1 ± 0.2	1.1	5.8	(15 °C)
DEPC–CH (3:1)	3.7 ± 0.2	4.0 ± 0.1	1.0	2.7	1.0
DEPC–CH (6:4)	7.8 ± 2.9	9.7 ± 0.3	2.3	6.7	2.4
DEPC–PA–CH (56:19:25)	23.6 ± 1.9	26.3 ± 2.1	5.5	18.3	2.4
	6.0 ± 0.4	12.9 ± 2.0	2.8	4.6	9.6 (15 °C)
asolectin	0.8 ± 0.8	21.2 ± 0.9	5.1	13.0	9.1
neutral lipid depleted asolectin	1.9 ± 0.1	8.1 ± 0.5	1.8	10.9	1.0
DOPC–PA–CH (56:19:25)	15.5 ± 6.6	43.1 ± 1.2	12.0	28.0	7.8
	6.1 ± 0.5	26.8 ± 0.3	5.5	14.5	6.6 (23 °C)
DOPC–CH (1:1)	1.2 ± 0.7	1.3 ± 0.8	0.5	4.0	0.6
DOPC–CH (2.24:1)	1.1 ± 0.7	3.3 ± 0.8	0.9	9.3	2.9
DOPC	1.5 ± 0.2	2.4 ± 0.4	0.5	6.5	1.7
DPePC(16:1*t*)-CH (3:1)	10.5 ± 3.5	13.4 ± 0.4	2.8	6.0	2.1
DPePC–DOPE–CH (56:19:25)	6.3 ± 0.4	9.2 ± 1.1	1.9	4.6	2.9
DPePC–PA–CH (56:19:25)	4.1 ± 1.0	14.2 ± 1.4	3.0	6.5	8.3
DLPC–PA–CH (56:19:25)	4.2 ± 0.8	9.3 ± 0.4	2.3	15.1	1.0

[a] Vesicle internal volume (IV) was defined as internal volume/total volume in units of microliters per milliliter. Equilibrium internal volume (EIV) was measured by allowing the influx reaction to proceed for 48 h at 4 °C. All influx reactions were carried out at 4 °C unless indicated in parentheses. All abbreviations are the same as those in Table II. [b] Response = [IV(+Carb) − IV(−Carb)]/EIV[AChR]. AChR concentration is defined as moles of ^{125}I-BgTx sites per liter of internal volume.

test for the level of significant difference between k_{co} and k_{pre} was carried out for each set of data. If the probability of the null hypothesis was equal to or less than 12%, i.e., k_{pre} was significantly smaller than k_{co}, the AChR in that particular membranes was said to be able to undergo the affinity-state interconversion. As shown in Table II, the ability of the AChR to undergo the affinity-state transition is highly dependent on the lipid environment in an all-or-none manner. Moreover, the effect of lipids was reversible since many functional vesicle samples (such as asolectin, DOPC–PA–CH, etc.) were prepared from the nonfunctional AChR–DOPC membranes by the re-reconstitution procedure.

Ion-Gating Activity of AChR in Vesicles of Different Lipid Composition. Sealed vesicles are required to detect the ion-

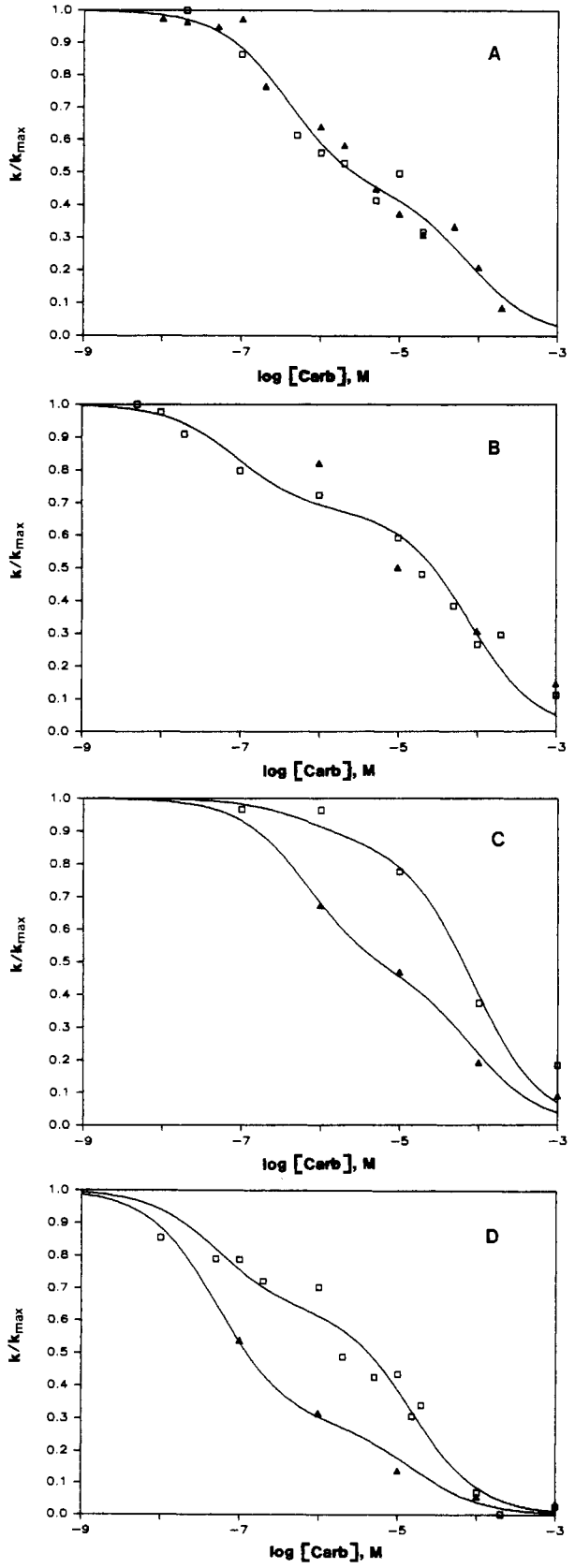

FIGURE 4: Inhibition of ^{125}I-BgTx binding rate by Carb. Solid lines were calculated from eq 1. (□) In the presence of Carb at concentrations indicated on the abscissa; (▲) AChR was preincubated with Carb first, and the binding was measured in the presence of Carb at the concentrations indicated. The concentration of Carb in the preincubation mixture, and all the parameters in eq 1 are listed in Table I. (A) Reconstituted AChR–DOPC membranes (lipid:protein ratio = 190); (B) re-reconstituted AChR–DOPC–CH membranes (lipid:protein ratio = 250, PC:CH ratio = 3); (C) re-reconstituted AChR–DOPC–PA–CH vesicles (PC:PA:CH ratio = 56:19:25); (D) reconstituted AChR–asolectin membranes (lipid:protein ratio = 150).

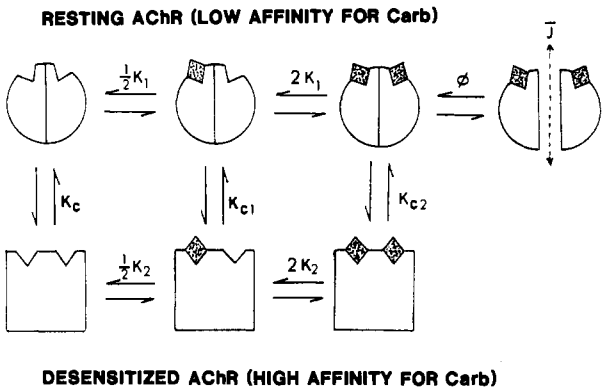

FIGURE 5: Schematic representation of the minimum molecular mechanism of AChR in which the shaded diamonds represent the carbamylcholine molecule.

gating activity of AChR-containing membranes when using the $^{86}Rb^+$ tracer technique. Therefore, vesicle samples with a lipid:protein ratio of 10 000 were reconstituted to promote the formation of large vesicles. Table III lists the results from the manual ion flux assays for various vesicle samples having different lipid compositions. The 30-s internal volume (microliters per milliliter) represents the internal volume of functional AChR-containing vesicles since the influx kinetics are fast (in the millisecond time domain), while the equilibrium internal volume represents the total internal volume including both AChR-free liposomes and AChR-containing vesicles. From the total internal volume and lipid concentration, it was possible to estimate the average diameter of the vesicles (Lichtenberg et al., 1981). Since the influx amplitude is affected by both AChR concentration (Wan & Lindstrom, 1985) and vesicle size, an index called "response" was calculated by normalizing the amounts of trapped Rb^+ to both AChR concentration and total internal volume. On the basis of a comparison of the influx amplitude and the response index, a vesicle sample with a response less than 0.03 μM^{-1} was said to be inactive since repeated experiments showed that a very low response value cannot be obtained reproducibly. It is apparent from Table III that all active samples contain cholesterol (or other sterols in the case of asolectin) and negatively charged phospholipids in addition to PC. The size of the vesicles as measured by the equilibrium internal volume is not positively correlated with the influx response; i.e., vesicles having a large size do not necessarily possess the ion-gating activity. As shown in Table III, the AChR–DEPC sample exhibited nonideal ion-flux behavior at 4 °C, which may be due to vesicle leakage for membranes in the gel phase.

Measurement of Membrane Fluidity. To establish a correlation between AChR function and membrane properties, spin-labeled fatty acid was incorporated into AChR-containing vesicles, and the membrane fluidity was measured by the order parameter of the spin-label in the membranes. Since high lipid:protein ratio samples were used in these measurements, the protein-perturbed component (Ellena et al., 1983) in the EPR spectra can be ignored. Figure 6 summarizes the results of affinity-state transition activity in a bar graph in which each square represents measurements for a specific lipid composition. For example, AChR in DOPC membranes did not manifest the affinity-state transition activity, while AChR in DEPC membranes, which are more rigid, was able to undergo the conformational change. In four PC–PA–CH samples containing different faty acyl chain configurations, only two of them with a moderate membrane fluidity (i.e., DOPC–PA–CH and DPePC–PA–CH) exhibited the affinity-state transition activity. The data demonstrate that the membranes

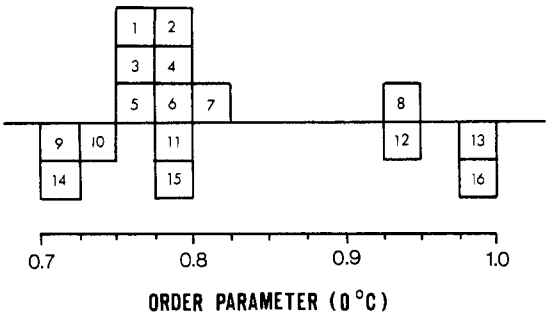

FIGURE 6: Correlation of the agonist affinity-state transition of AChR and membrane fluidity. Each block in the graph represents measurements for one specific lipid composition. All samples above the horizontal line are active, while all samples below the line are inactive (see Table II). The lipid compositions of the samples are as follows: (1) neutral lipid depleted asolectin; (2) DOPC–CH (1:1); (3) DOPC–PA–CH (56:19:25); (4) DPePC–DOPE–CH (56:19:25); (5) asolectin; (6) *Torpedo* native lipids; (7) DPePC–PA–CH (56:19:25); (8) DEPC; (9) DOPC; (10) CH-depleted *Torpedo* native lipids; (11) DOPC–CH (2.24:1); (12) DEPC–PA–CH (56:19:25); (13) DEPC–CH (3:1); (14) DLPC–PA–CH (56:19:25); (15) DPePC–CH (3:1); (16) DEPC–CH (6:4).

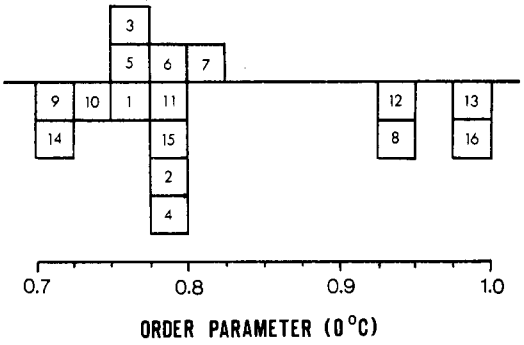

FIGURE 7: Correlation of AChR-mediated ion flux and membrane fluidity. All samples above the horizontal line are active, while all samples below the line are inactive (see Table III). Sample numbering is the same as in Figure 6.

in which AChR is capable of undergoing conformational change possess a membrane fluidity falling within a small window on the order parameter scale. An appropriate membrane fluidity appears to be a necessary but not sufficient condition for the conformational transition. As for the ion-gating activity of AChR, a similar fluidity dependence was observed in which all active vesicle samples possessed similar membrane fluidity (Figure 7). All vesicle samples that gave a flux response were able to undergo the conformational change, but the converse was not true.

The temperature dependence of membrane fluidity was studied for three different lipid compositions (Figure 8). For AChR in DOPC–PA–CH or asolectin membranes, the vesicles were completely functional in the range of 4–23 °C (Tables II and III). In contrast, DEPC–PA–CH membranes exhibited a sharp phase transition at about 7 °C, and AChR in this membrane was active at 15 °C but not at 4 °C (Tables II and III).

Effects of Removing Cholesterol and Neutral Lipids from Native Membranes and Asolectin Membranes. Cholesterol and other neutral lipids were removed from extracted native lipids and asolectin by silica gel column chromatography (Bergelson, 1980). AChR's were then re-reconstituted into vesicles containing these modified lipids. As shown in Figure 6, removal of neutral lipids from asolectin did not significantly change the membrane fluidity (an increase from 0.753 to 0.771). AChR in neutral lipid depleted asolectin vesicles still manifested the agonist affinity-state transition activity, while

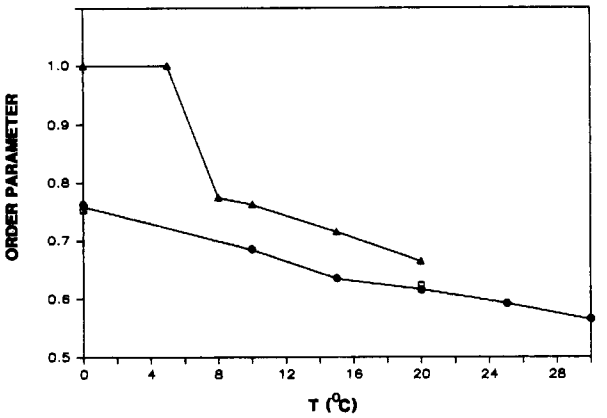

FIGURE 8: Temperature dependence of membrane fluidity. (●) DOPC–PA–CH vesicles; (▲) DEPC–PA–CH vesicles; (□) asolectin vesicles.

the ion-gating activity no longer remained (Tables II and III). In contrast, removal of cholesterol from *Torpedo* native lipids modified the membrane fluidity to a larger extent (a decrease from 0.800 to 0.749). AChR's in cholesterol-depleted *Torpedo* lipid vesicles exhibited neither the state transition nor ion-gating activities (Tables II and III).

Discussion

The experimental data presented here provide new insights into the functional implications of protein–lipid interactions. First, dissociation constants of agonist from AChR are not significantly affected by the change of lipid environment. This conclusion is consistent with the demonstration that the agonist binding sites are located on the extracellular domain well above the surface of membranes (Stroud, 1983). Therefore, the binding site conformation is not changed by the change of molecular interaction at the lipid–protein interface. In contrast, it has been reported that a marked increase in the apparent Carb dissociation constant was observed with increasing chain length of saturated PC's (Criado et al., 1984). This result was obtained by assuming that all AChR's were in one affinity state, and thus the apparent Carb dissociation constant was expected to be equal to EC_{50}. From the computer simulation such as those shown in Figure 4, it is obvious that the data cannot be fitted by a single-state model. Two different states of AChR, one with low affinity and the other with high affinity, coexist in membranes even in the absence of agonist (Figure 5). Therefore, a two-state model (eq 1) should be used to fit the toxin binding kinetic data.

Second, in contrast to the invariance of Carb dissociation constants in different membranes, the change in the fraction of AChR in the low-affinity state after preincubation with Carb was different for AChR in different membranes (Table I). The value of F_a clearly affects the shape of the dose–response curve in a more profound way than the values of K_1 and K_2 (Figure 4). The ability of AChR to undergo the low- to high-affinity-state transition was dramatically changed in different lipid environments, which implies that the conformational-state interconversion is dependent on the nature of the lipid environment.

The affinity-state transition involves conformational changes that lead to AChR desensitization (Neubig et al., 1982; Heidmann et al., 1983). Such a dynamic process is expected to be influenced by the dynamic structure of membranes since the ionic channel is located within the membranes. This expectation is confirmed by the results in Figure 6, which shows that an appropriate membrane fluidity is a necessary condition for the affinity-state transition. At 4 °C, AChRs in mem-

branes with either a very low fluidity or a very high fluidity are not capable of undergoing the conformational transition. Our experimental results are consistent with the hypothesis that membrane protein conformational changes require an optimal membrane fluidity and the conformational transition will not occur in membranes with either very low or very high fluidity. In support of this hypothesis, it has been reported that the conformational transition of myoglobin is highly dependent on the solvent viscosity (Beece et al., 1980). The Kramers equation

$$k^* = \left(\frac{A}{\eta} + A^0\right) \exp(-H^*/RT) \qquad (2)$$

was used to fit their experimental data, in which A and A^0 are system-dependent constants and η is the solvent viscosity. This dynamic model describes the barrier governing the transition between two states as a gate that opens and closes rather than as a stationary potential barrier described by the conventional transition-state theory. Thus, transition between substates is achieved by structural fluctuation which is a viscosity (or damping) dependent process. The Kramers equation has also been applied to enzymatic reactions (Gavish & Werber, 1979) and the photocycle of bacteriorhodopsin (Beece et al., 1981).

In the present studies, an equilibrium approach was used to determine the conformational transition; i.e., the transition from low-affinity state to high-affinity state after preincubation of AChR with Carb for 20 min was observed only if the transition rate constant was above a certain threshold value. The data shown in Figure 6 can be qualitatively described by the Kramers equation in the low fluidity region. In the high fluidity region, however, the Kramers equation no longer applies to our system because no conformational transition is observed for AChR in membranes with a very small order parameter. Theoretical analysis also indicates that the Kramers theory holds only in the high damping limit (Gavish, 1980). Comparison of Mössbauer and X-ray investigations with computer simulation has shown that protein dynamics at a physiological temperature is an overdamped diffusion-like motion in a restricted space (Parak & Knapp, 1984), which implies that the protein conformational transition is not a consequence of high-frequency relaxation. In the case of multisubunit membrane proteins, a moderate membrane fluidity may be required to maintain the integrity of quaternary structure and prevent energy dissipation due to high-frequency fluctuations. Ideally, it would be desirable to measure the motional property of the boundary lipid domain. In our experiments, we only measured the fluidity of the bulk-phase lipid domain as a first approximation. As mentioned under Results, we used both low and high lipid:protein ratio samples for studying the conformational transition property of AChR. It is justified that AChR has the same functional property in both systems since the lipid:protein ratio is well above the number of lipid molecules surrounding AChR [see also Hesketh et al. (1976), Knowles et al. (1979), and Ellena et al. (1983)].

In contrast to the above discussion, it has been argued that membrane fluidity is not an important physiological regulator of membrane enzymes since no correlation was observed between the enzymatic activity of Ca^{2+}-ATPase and the order parameter of membranes in the range of 0.5–0.6 at 37 °C (East et al., 1984). Although only a narrow range of membrane fluidity within the liquid-crystalline phase was examined, membranes in the gel phase supported only very low ATPase activity (East et al., 1984), which is consistent with our observations. If more samples were examined for Ca^{2+}-ATPase in the low fluidity region, it might be possible to reveal the effect of fluidity on ATPase activity. Recently, it was reported that the tryptic susceptibility of Ca^{2+}-ATPase was correlated with membrane fluidity (Blazyk et al., 1985), from which it was concluded that the conformational fluctuation of Ca^{2+}-ATPase is dependent on the phase change of sarcoplasmic reticulum membranes.

Third, the activation of the AChR cation channel also involves conformational changes, and it is not surprising that the AChR-mediated ion flux requires an optimal membrane fluidity as shown in Figure 7. In addition to the fluidity requirement, the ion-gating activity also requires the presence of cholesterol and negatively charged phospholipids in the membranes (Table III; Ochoa et al., 1983; Criado et al., 1984). The size difference of various vesicle samples cannot fully explain the effects of lipid composition on the AChR-mediated ion flux response. The results indicate that a conformational transition (or structural flexibility) is not sufficient for reaching the open-channel state. Other factors besides fluidity are also critical for AChR function. It has been proposed that the ion channel is composed of five amphipathic α-helices on the basis of amino acid sequence analysis (Finer-Moore & Stroud, 1984; Guy, 1984). It is apparent that both dynamic and static structures of membrane proteins should be considered when structure–function relationships are studied. Although AChR in some lipid environments has the dynamic capability to undergo conformational changes, it is possible that these receptors do not have the correct static structure necessary for forming an ionic channel. We propose that cholesterol, and perhaps negatively charged phospholipids, may stabilize the amphipathic helical structure in AChR which defines the potential ionic channel and which is responsible for channel opening when conformational change is induced by agonist binding. It has been reported that cholesterol in membranes does increase the helical content in membrane proteins of cholesterol-modified human erythrocyte membranes (Rooney et al., 1984). As for the specific role of negatively charged phospholipids in interaction with membrane proteins, it is also possible that they may exert their effects through membrane surface charge density in the way that the local ionic concentration sensed by the channel is determined by both the bulk ionic concentration and the lipid surface potential (Bell & Miller, 1984; Cristiansson et al., 1985).

Therefore, three conditions have to be satisfied to fully support AChR functions, including an appropriate membrane fluidity, the presence of cholesterol, and the presence of negatively charged phospholipids (such as PA). The lipid compositional requirement is consistent with the fact that high percentages of cholesterol and phosphatidylserine are found in the electroplax membranes (Gonzalez-Ros et al., 1982) and that AChR interacts strongly with sterol molecules and PA in membrane bilayers (Ellena et al., 1983). It is possible that these membrane lipids are selected from the bulk phase by interacting strongly with AChR, thus providing an optimal environment for AChR functions. Since different lipids have different affinity for AChR, the lipid composition of the shell in contact with AChR will differ from the lipid composition of the bulk phase. Nevertheless, such a difference will not obscure the qualitative interpretation of the lipid compositional requirement as none of the lipids we used is excluded from AChR or is exclusively surrounding AChR (Ellena et al., 1983). In a less biologically relevant system, i.e., AChR in the monolayer of pure lipids at the air–water interface, strong interaction with cholesterol was also reported (Popot et al., 1978). Using the monolayer technique, Schubert and co-

workers (Klappauf & Schubert, 1979; Schubert & Boss, 1982) examined the interaction of various membrane lipids with band 3–protein from human erythrocyte membranes and found that cholesterol interacted more strongly with band 3–protein than other membrane lipids. It is interesting to notice that cholesterol is also the most abundant lipid species in the human erythrocyte membranes (Grunze et al., 1980) and cholesterol may be critical for some of the biological functions in erythrocyte membranes such as ionic channel functions.

Our experimental results have shown that the AChR conformational transition and its ion channel conformation are highly dependent on the lipid environments. According to the microscopic reversibility principle, the agonist-induced conformational changes must, in turn, affect the molecular interaction at the lipid–protein interface. This is confirmed by the results obtained by Gonzalez-Ros et al. (1983). It was reported that the susceptibility of a fluorophore at the bilayer region of AChR to hydrophobic quenching molecules decreased only in the presence of agonist, and the effect was reversible by removing the agonist.

The manual ion flux assay we used is an equilibrium assay which provides only qualitative measurement of AChR channel activity. It is ideally suited for "all-or-none" measurement of AChR activity. Analogous to the lipid environment dependence of state transition rate, the kinetic behavior of AChR activation can also be affected by the change of lipid environment. The rate constant of ion translocation through the channel ($\bar{J}$, see Figure 5) and/or the equilibrium constant of channel closing (ϕ) can be dramatically affected in different lipid environments on the basis of kinetic measurement of Rb^+ influx (T. M. Fong and M. G. McNamee, unpublished results). It has been reported that AChR reconstituted into a planar lipid bilayer manifested similar single-channel conductance as those observed in intact rat and frog muscle membranes (Schindler & Quast, 1980; Nelson et al., 1980; Boheim et al., 1981). Since the single-channel conductance is directly related to the rate constant of ion translocation through the cation channel (Hess et al., 1984), it is more likely that the value of ϕ, which is also an equilibrium constant of a conformational transition reaction, is modulated by the dynamic structure of lipid bilayers.

We have measured AChR activities at 4 °C in most of the experiments. Since membrane fluidity is a temperature-dependent function, we tested the two hypotheses stated above by studying the state transition and ion gating at two very different temperatures. DEPC–PA–CH membranes satisfy the lipid composition requirement, but it is in the gel phase at 4 °C. It is predicted that if the membrane fluidity is modified to about the same range as DOPC–PA-CH membranes by increasing temperature, AChR in that lipid environment will be completely functional. This is confirmed by doing the ion flux assay and the state transition measurement at 15 °C (Tables II and III). It should be pointed out that the fluidity effect is best illustrated at constant temperature for different membrane samples. When the temperature is manipulated, the internal molecular motion of protein itself is affected since the Kramers equation states that the rate constant is a function of both temperature and medium viscosity, resulting in the introduction of a second variable (temperature) in addition to membrane fluidity. In spite of these complications, it is clearly demonstrated that the physical state of membranes does modulate AChR activities.

To test the essential requirement of cholesterol (or other sterol molecules), cholesterol or neutral lipids were depleted from *Torpedo* native lipids and asolectin before reconstitution. As expected, removal of cholesterol resulted in a significant change in membrane fluidity of the native membranes, and AChR in such modified membranes was not capable of undergoing the conformational changes. In the case of neutral lipid depleted asolectin membranes, the state transition property still remained since the membrane fluidity was not significantly modified, while the ion-gating activity was lost. Kilian et al. (1980) also reported that removal of neutral lipids from asolectin resulted in a dramatic decrease in the AChR-mediated ion flux response.

In summary, an optimal fluidity hypothesis is proposed to account for the fluidity dependence of AChR conformational transitions. However, the dynamic capability of AChR to undergo conformational changes per se does not guarantee a priori formation of an ionic channel. It was found that conformational change is only a necessary condition for the ion-gating activity of AChR. It is proposed that the amphipathic α-helical structure in AChR is stabilized by the interaction with certain specific lipids such as cholesterol and negatively charged phospholipids. These static molecular interactions are essential to the ion channel conformation while the dynamic processes of internal molecular motions will control the opening and closing of the ion channel.

ACKNOWLEDGMENTS

We are indebted to Amy Yee, Charlie Richardson, and Drs. Owen Jones and Julie Earnest for their valuable suggestions and discussions. We also thank Peter Louie for preparing electroplax membranes and technical assistance.

Registry No. CH, 57-88-5; DLPC, 6542-05-8; DOPC, 10015-85-7; DOPE, 2462-63-7; Rb, 7440-17-7; carbamylcholine, 462-58-8.

REFERENCES

Andreasen, T. J., & McNamee, M. G. (1980) *Biochemistry 19*, 4719–4726.

Anholt, R., Fredkin, D. R., Deerinck, T., Ellisman, M., Montal, M., & Lindstrom, J. (1982) *J. Biol. Chem. 257*, 7122–7134.

Barrantes, F. J. (1983) *Int. Rev. Neurobiol. 24*, 259–341.

Beece, D., Eisenstein, L., Frauenfelder, H., Good, D., Marden, M. C., Reinisch, L., Reynolds, A. H., Sorensen, L. B., & Yue, K. T. (1980) *Biochemistry 19*, 5147–5157.

Beece, D., Bowne, S. F., Czege, J., Eisenstein, L., Frauenfelder, H., Good, D., Marden, M. C., Marque, J., Ormos, P., Reinisch, L., & Yue, K. T. (1981) *Photochem. Photobiol. 33*, 517–522.

Bell, J., & Miller, C. (1984) *Biophys. J. 45*, 279–287.

Bergelson, L. D. (1980) in *Lipid Biochemical Preparations* (Bergelson, L. D., Ed.) pp 24–28, Elsevier/North-Holland, New York.

Blazyk, J., Wu, C. J., & Wu, S. C. (1985) *J. Biol. Chem. 260*, 4845–4849.

Bligh, E. G., & Dyer, W. J. (1959) *Can. J. Biochem. Physiol. 37*, 911–917.

Boheim, G., Hanke, W., Barrantes, F. J., Eibl, H., Sakmann, B., Fels, G., & Maelicke, A. (1981) *Proc. Natl. Acad. Sci. U.S.A. 78*, 3586–3590.

Brotherus, J. R., Griffith, O. H., Brotherus, M. O., Jost, P. C., Silvius, J. R., & Hokin, L. E. (1981) *Biochemistry 20*, 5261–5267.

Changeux, J.-P., Devillers-Thiery, A., & Chemouilli, P. (1984) *Science (Washington, D.C.) 225*, 1335–1345.

Christiansson, A., Eriksson, L. E. G., Westman, J., Demel, R., & Weislander, A. (1985) *J. Biol. Chem. 260*, 3984–3990.

Criado, M., Eibl, H., & Barrantes, F. J. (1984) *J. Biol. Chem. 259*, 9188–9198.
Dalziel, A. W., Rollins, E. S., & McNamee, M. G. (1980) *FEBS Lett. 122*, 193–196.
De Lean, A., Munson, P. J., & Rodbard, D. (1978) *Am. J. Physiol. 235 (2)*, E97–E102.
Devaux, P. F. (1983) *Biol. Magn. Reson. 5*, 183–299.
East, J. M., Jones, O. T., Simmonds, A. C., & Lee, A. G. (1984) *J. Biol. Chem. 259*, 8070–8071.
East, J. M., Melville, D., & Lee, A. G. (1985) *Biochemistry 24*, 2615–2623.
Ellena, J. F., Blazing, M. A., & McNamee, M. G. (1983) *Biochemistry 22*, 5523–5535.
Finer-Moore, J., & Stroud, R. M. (1984) *Proc. Natl. Acad. Sci. U.S.A. 81*, 155–159.
Gaffney, B. J. (1976) in *Spin Labeling: Theory and Applications* (Berliner, L. J., Ed.) pp 567–571, Academic Press, New York.
Gavish, B. (1980) *Phys. Rev. Lett. 44*, 1160–1163.
Gavish, B., & Werber, M. M. (1979) *Biochemistry 18*, 1269–1275.
Gonzalez-Ros, J. M., Llanillo, M., Paraschos, A., & Martinez-Carrion, M. (1982) *Biochemistry 21*, 3467–3474.
Gonzalez-Ros, J. M., Farach, M. C., & Martinez-Carrion, M. (1983) *Biochemistry 22*, 3807–3811.
Griffith, O. H., Brotherus, J. R., & Jost, P. C. (1982) in *Lipid–Protein Interactions* (Jost, P. C., & Griffith, O. H., Eds.) Vol. 2, pp 225–238, Wiley, New York.
Grunze, M., Forst, B., & Deuticke, B. (1980) *Biochim. Biophys. Acta 600*, 860–869.
Guy, H. R. (1984) *Biophys. J. 45*, 249–261.
Heidmann, T., Bernhardt, J., Neumann, E., & Changeux, J.-P. (1983) *Biochemistry 22*, 5452–5459.
Hesketh, T. R., Smith, G. A., Housley, M. D., McGill, K. A., Birdsall, N. J. M., Metcalfe, J. C., & Warren, G. B. (1976) *Biochemistry 15*, 4145–4151.
Hess, G. P., Cash, D. J., & Aoshima, H. (1983) *Annu. Rev. Biophys. Bioeng. 12*, 443–473.
Hess, G. P., Kolb, H.-A., Lauger, P., Schoffeniels, E., & Schwarze, W. (1984) *Proc. Natl. Acad. Sci. U.S.A. 81*, 5281–5285.
Kilian, P. L., Dunlap, C. R., Mueller, P., Schell, M. A., Huganir, R. L., & Racker, E. (1980) *Biochem. Biophys. Res. Commun. 93*, 409–414.
Klappauf, E., & Schubert, D. (1979) *Hoppe-Seyler's Z. Physiol. Chem. 360*, 1225–1235.
Knowles, P. F., Watts, A., & Marsh, D. (1979) *Biochemistry 18*, 4480–4487.
Lichtenberg, D., Freire, E., Schmidt, C. F., Barenholz, Y., Felgner, P. L., & Thompson, T. E. (1981) *Biochemistry 20*, 3462–3467.
London, E., & Feigenson, G. W. (1981) *Biochemistry 20*, 1939–1948.
Lowry, O. H., Rosebrough, N. J., Farr, A. L., & Randall, R. J. (1951) *J. Biol. Chem. 193*, 265–275.
Marsh, D. (1983) *Trends Biochem. Sci. (Pers. Ed.) 8*, 330–333.
McClare, C. W. (1971) *Anal. Biochem. 39*, 527–530.
McNamee, M. G., & Ochoa, E. L. M. (1982) *Neuroscience (Oxford) 7*, 2305–2319.
McNamee, M. G., Jones, O. T., & Fong, T. M. (1986) in *Ion Channel Reconstitution* (Miller, C., Ed.) pp 231–273, Plenum Press, New York.
Nelson, N., Anholt, R., Lindstrom, J., & Montal, M. (1980) *Proc. Natl. Acad. Sci. U.S.A. 77*, 3057–3061.
Neubig, R. R., Boyd, N. D., & Cohen, J. B. (1982) *Biochemistry 21*, 3460–3467.
Ochoa, E. L. M., Dalziel, A. W., & McNamee, M. G. (1983) *Biochim. Biophys. Acta 727*, 151–162.
Parak, F., & Knapp, E. W. (1984) *Proc. Natl. Acad. Sci. U.S.A. 81*, 7088–7092.
Pink, D. A., Chapman, D., Laidlaw, D. J., & Wiedmer, T. (1984) *Biochemistry 23*, 4051–4058.
Pjura, W. J., Kleinfeid, A. M., Klausner, R. D., & Karnovsky, M. J. (1982) *Biophys. J. 37*, 69–71.
Popot, J.-L., & Changeux, J.-P. (1984) *Physiol. Rev. 64*, 1162–1239.
Popot, J.-L., Demel, R. A., Sobel, A., Van Deenen, L. L. M., & Changeux, J.-P. (1978) *Eur. J. Biochem. 85*, 27–42.
Quast, U., Schimerlik, M., Lee, T., Witzemann, V., Blanchard, S., & Raftery, M. A. (1978) *Biochemistry 17*, 2405–2414.
Rooney, M. W., Lange, Y., & Kauffman, J. W. (1984) *J. Biol. Chem. 259*, 8281–8285.
Sandermann, H., Jr. (1983) *Trends Biochem. Sci. (Pers. Ed.) 8*, 408–411.
Scandella, C., Campisi, J., Elhai, J., & Selak, M. (1982) *Biophys. J. 37*, 16–17.
Schindler, H., & Quast, U. (1980) *Proc. Natl. Acad. Sci. U.S.A. 77*, 3052–3056.
Schmidt, J., & Raftery, M. A. (1973) *Anal. Biochem. 52*, 349–354.
Schubert, D., & Boss, K. (1982) *FEBS Lett. 150*, 4–8.
Shaw, J. M., Henry, J. E., Shaw, K. V., & Konigsberg, I. R. (1983) *Biochim. Biophys. Acta 733*, 1–14.
Silvius, J. R., McMillen, D. A., Saley, N. D., Jost, P. C., & Griffith, O. H. (1984) *Biochemistry 23*, 538–547.
Simmonds, A. C., Rooney, E. K., & Lee, A. G. (1984) *Biochemistry 23*, 1432–1441.
Stroud, R. M. (1983) *Neurosci. Comment. 1*, 124–138.
Walker, J. W., Lukas, R. J., & McNamee, M. G. (1981) *Biochemistry 20*, 2191–2199.
Walker, J. W., Takeyasu, K., & McNamee, M. G. (1982) *Biochemistry 21*, 5384–5389.
Wan, K. K., & Lindstrom, J. M. (1985) *Biochemistry 24*, 1212–1221.
Warren, G. B., Houslay, M. D., Metcalfe, J. C., & Birdsall, N. J. M. (1975) *Nature (London) 255*, 684–687.
Weber, M., David-Pfeuty, T., & Changeux, J.-P. (1975) *Proc. Natl. Acad. Sci. U.S.A. 72*, 3443–3447.
Weiland, G., Georgia, B., Lappi, S., Chignell, C. F., & Taylor, P. (1977) *J. Biol. Chem. 252*, 7648–7656.
Whetton, A. D., Gordon, L. M., & Houslay, M. D. (1983a) *Biochem. J. 210*, 437–449.
Whetton, A. D., Gordon, L. M., & Houslay, M. D. (1983b) *Biochem. J. 212*, 331–338.
Yguerabide, J., & Yguerabide, E. E. (1985) in *The Enzymes of Biological Membranes* (Martonosi, A. N., Ed.) 2nd ed., Vol. 1, pp 393–420, Plenum Press, New York.
Yoshida, Y., Furuya, E., & Tagawa, K. (1980) *J. Biochem. (Tokyo) 88*, 463–468.